


 Cite this: *Nanoscale*, 2024, **16**, 1792

Interaction of graphene and WS₂ with neutrophils and mesenchymal stem cells: implications for peripheral nerve regeneration†

 Domenica Convertino,[‡] ^{*,†,a} Martina Nencioni,^{‡,b} Lara Russo,^{‡,b} Neeraj Mishra,^{a,c} Vesa-Matti Hiltunen,^{a,c} Maria Sofia Bertilacchi,^b Laura Marchetti,^{a,b} Chiara Giacomelli,[‡] ^{*,b} Maria Letizia Trincavelli^{§,b} and Camilla Coletti ^{*,§,a,c}

Graphene and bidimensional (2D) materials have been widely used in nerve conduits to boost peripheral nerve regeneration. Nevertheless, the experimental and commercial variability in graphene-based materials generates graphene forms with different structures and properties that can trigger entirely diverse biological responses from all the players involved in nerve repair. Herein, we focus on the graphene and tungsten disulfide (WS₂) interaction with non-neuronal cell types involved in nerve tissue regeneration. We synthesize highly crystalline graphene and WS₂ with scalable techniques such as thermal decomposition and chemical vapor deposition. The materials were able to trigger the activation of a neutrophil human model promoting Neutrophil Extracellular Traps (NETs) production, particularly under basal conditions, although neutrophils were not able to degrade graphene. Of note is that pristine graphene acts as a repellent for the NET adhesion, a beneficial property for nerve conduit long-term applications. Mesenchymal stem cells (MSCs) have been proposed as a promising strategy for nerve regeneration in combination with a conduit. Thus, the interaction of graphene with MSCs was also investigated, and reduced viability was observed only on specific graphene substrates. Overall, the results confirm the possibility of regulating the cell response by varying graphene properties and selecting the most suitable graphene forms.

Received 29th September 2023,

Accepted 10th December 2023

DOI: 10.1039/d3nr04927b

rsc.li/nanoscale

1 Introduction

In the last few years of studies on nerve injury, biocompatible scaffolds have increasingly been investigated for their capability of supporting the regeneration of the damaged nerve. Many works have reported on how the use of conduits could beneficially affect the healing process and ameliorate the outcome of nerve regeneration, thanks to an optimal combination of specific physiochemical, mechanical, and electrical properties.^{1–3} Also, these structures can be functionalized with biological materials such as growth factors, extracellular vesicles and cells, to further support regeneration.^{4,5}

Regeneration conduits are mainly composed of biocompatible natural and synthetic materials, endowed with mechanical resistance, electrical conductivity, and topographical guiding features.^{1,6} The interactions of these materials with neuronal cells as well as Schwann cells, *i.e.* the main cells that build up nerves, are nowadays well documented;^{7–10} the effects that they exert on neuronal differentiation and neurite outgrowth have been studied down to the molecular detail.^{11–13} Nevertheless, injured nerve regions typically include several other cell types playing a role in the regeneration pathways.^{4,14–18} An example is constituted by macrophages and other immune system cells like neutrophils.¹⁹ Indeed, almost immediately after the damage, Schwann cells dissociate from axons, dedifferentiate, and secrete cytokines and chemokines,² prompting the recruitment of neutrophils, the first immune cell type that arrives at the site of inflammation from the bloodstream. They infiltrate the tissue within 8 hours after damage and carry out their immune action *via* three main mechanisms: phagocytosis, degranulation and NETosis.^{20,21} NETosis is a process of programmed cell death characterized by the release of a network of chromatin, histones and proteins from all types of neutrophil granules to the extracellular space. Initially reported for their ability to form a physical trap for pathogens (from which

^aCenter for Nanotechnology Innovation @ NEST, Istituto Italiano di Tecnologia, Piazza San Silvestro 12, Pisa, Italy. E-mail: domenica.convertino@iit.it, camilla.coletti@iit.it

^bDepartment of Pharmacy, University of Pisa, Via Bonanno 6, Pisa, Italy. E-mail: chiara.giacomelli@unipi.it

^cGraphene Labs, Istituto Italiano di Tecnologia, Via Morego 30, Genova, Italy

†Electronic supplementary information (ESI) available. See DOI: <https://doi.org/10.1039/d3nr04927b>

‡These authors equally contributed to the work.

§These authors share last authorship.



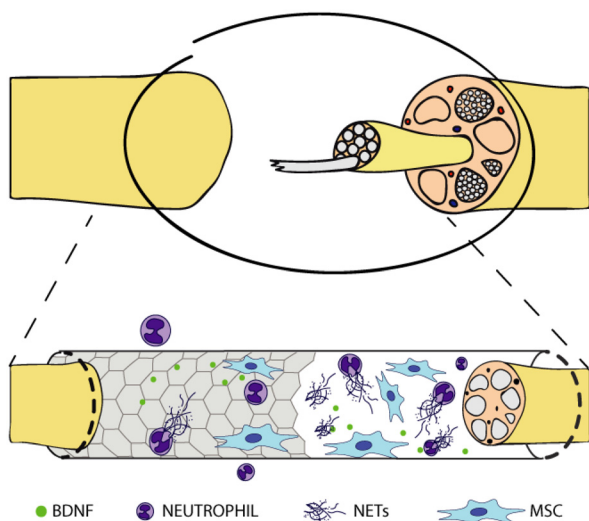


Fig. 1 Graphene-coated nerve conduit for nerve regeneration. Interaction with neutrophils and mesenchymal stem cells.

peripheral nerve regeneration has been scarcely unravelled, especially concerning the one synthesized by CVD. Yet, to achieve an optimal pro-regenerative performance of 2D material-based conduits, the interaction of the 2D material with the different cell types involved in peripheral nerve injury needs to be understood. Indeed, the implantation of foreign materials may reinforce the establishment of a local inflammatory micro-environment, which leads to the recruitment of even more cells like neutrophils or MSCs, influencing the correct activation of the resulting immune cascade.⁷⁰ Moreover, this microenvironment could lead to a non-specific destruction of the adjacent healthy tissue or of the biomaterial and an improper integration between them.⁷¹ Furthermore, both graphene and carbon nanotubes may undergo neutrophil-mediated degradation.^{72,73}

In this study, we prepared different graphene substrates, namely CVD graphene on sapphire, epitaxial graphene on SiC *via* thermal decomposition, both as-grown and hydrogen intercalated (H-intercalated), and CVD graphene grown on copper and transferred on glass, along with CVD monolayer tungsten disulfide (WS₂) on sapphire, as an alternative to graphene. Subsequently, we tested them as culture substrates for human neutrophils and human MSCs to shed light on the immune and pro-regenerative responses they could stimulate when adopted as nerve conduit materials in the context of peripheral nerve regeneration (Fig. 1). No external stimulation was applied, since we were mostly interested in the intrinsic properties of the materials, to assess how surface chemistry and electrical conductivity *per se* could affect the cell behaviour.

2 Materials and methods

2.1 Substrate preparation and characterization

Graphene on glass (G glass) was obtained by transferring on glass coverslips graphene grown on copper (Cu).

Polycrystalline monolayer graphene was synthesized on electro-polished Cu foil (purity 99.8%, 46365, Alfa-Aesar) using a 4" Aixtron BM Pro cold-wall reactor as previously described.^{11,55} Graphene was transferred on glass coverslips using a standard wet etching process with ammonium persulfate (APS, 248614, Sigma Aldrich) as copper etchant.¹¹

Graphene was grown on the silicon face (Si-face) of hydrogen etched silicon carbide (6H n-type SiC, TankeBlue Semiconductor, China) in an Aixtron HT-BM reactor *via* thermal decomposition (G SiC). Quasi-free standing monolayer graphene (G SiC Hint) was obtained starting from buffer layer graphene obtained *via* thermal decomposition and subsequently intercalated under a hydrogen-rich atmosphere.^{7,74}

Monolayer graphene on sapphire (Hangzhou Silan Microelectronics, China) with bilayer patches (G sapp) was synthesized *via* CVD in the same Aixtron HT-BM reactor adopted to grow graphene on SiC.^{62,75}

Monolayer tungsten disulphide (WS₂) was grown directly on 2-inch *c*-plane sapphire wafer (Hangzhou Silan Microelectronics, China) *via* a low-pressure CVD process using tungsten trioxide (WO₃, 204781, Sigma Aldrich) and sulphur (S, 213292, Sigma Aldrich) as solid precursors in a horizontal hot-wall furnace (Carbolite Gero). The growth was performed at 950 °C for 10 minutes under a pressure of 6 mbar and 420 sccm flow of a gas mixture of 3% H₂ in argon.^{62,76}

The controls adopted in the experiments were: (i) bare glass coverslips (Glass, Corning, USA); (ii) hydrogen etched Si-face SiC dices (the same substrates where graphene was grown) (SiC);^{7,77} (iii) sapphire dices (Sapp).

When graphene and WS₂ samples needed to be cut to fit the culture well plates, the surfaces were protected with a polymer (PMMA, 679.04, All-resist) deposited by spin-coating to reduce the scratch formation. The polymer was then removed by immersing the samples in acetone for at least 2 h and rinsing them with isopropanol. The size of all the samples was about 4 × 4 mm².

Before cell culture, all substrates were sterilized by 30 minutes immersion in 96% ethanol and then rinsed several times with deionized (DI) water.

The topography, quality and number of layers of graphene and WS₂ were assessed by both atomic force microscopy (AFM) and Raman spectroscopy.

2.2 HL60 cell culture and differentiation

The human promyelocytic leukaemia (HL60) cell line was used as a cellular model to study NETosis on the 2D material surfaces.⁷⁸ HL60 cells were obtained from the European Collection of Authenticated Cell Cultures (ECACC, UK Health Security Agency, UK; 98070106). Cells were cultured in RPMI-1640 culture medium (Corning™ RPMI 1640 medium without L-glutamine; 15-040-CV) supplemented with 10% fetal bovine serum (Corning™ 35-016-CV), 2 mM L-glutamine (Euroclone ECB 3000D), 1% penicillin/streptomycin solution (Corning™ 30-002-CI) and incubated at 37 °C in 5% CO₂. The cells were maintained in suspension at 100 000–1 000 000 cells per ml confluency. The differentiation of HL60 to neutrophil-



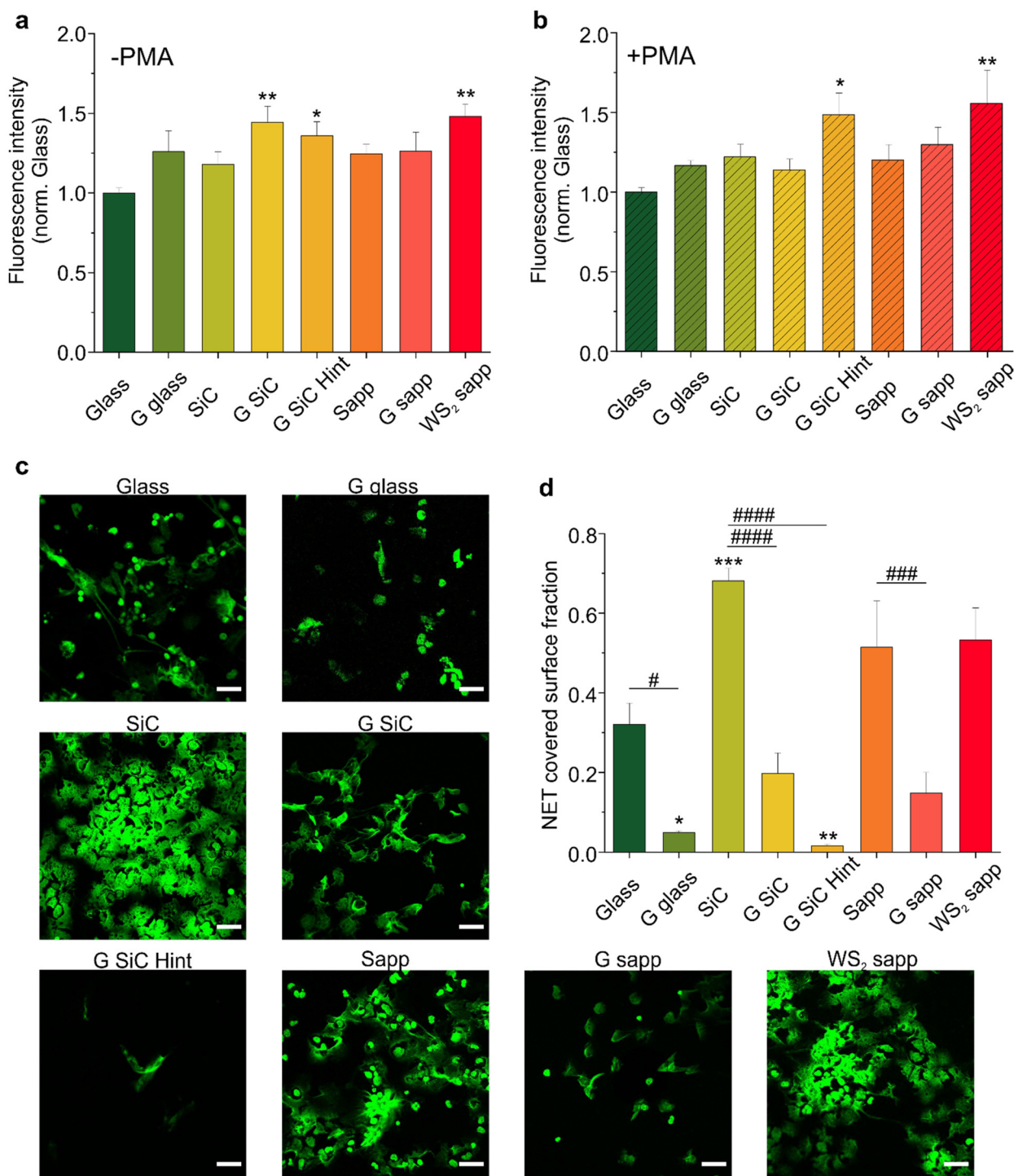


Fig. 2 Neutrophil-like differentiated HL60 (dHL60) cultured on graphene transferred on glass (G glass), graphene on SiC (G SiC), graphene on SiC hydrogen intercalated (G SiC Hint), graphene on sapphire (G sapp), WS₂ on sapphire (WS₂ sapp) and control substrates: glass, SiC and sapphire (Sapp). (a and b) Quantification of the mean fluorescence intensity of NETs released as extracellular DNA by Sytox green staining of dHL60 after a 4 h incubation with graphene and WS₂ in the absence (a) or presence of PMA (b). Data of two independent experiments were reported as mean \pm standard error of the mean (s.e.m.). Data are expressed as the fluorescence intensity versus the glass control set to 1. One-way ANOVA with Dunnett *post hoc* test was used for statistical significance with respect to glass control, with * $p < 0.05$, ** $p < 0.01$. No statistical significance (one-way with Sidak *post hoc* test, $p < 0.05$) was observed between graphene and WS₂ with respect to the substrate on which they were grown (SiC, sapphire) or transferred (Glass). (c) Representative confocal images of fixed NETs released from PMA-activated neutrophils adhered to each 2D material. NETs were identified as positive for cell impermeable Sytox green. Scale bar: 20 μm . (d) Quantitative analysis of NET covered surface fraction of the 2D materials. Data of two independent experiments are reported as mean \pm s.e.m. One-way ANOVA with Dunnett *post hoc* test was used for statistical significance with respect to glass control, with * $p < 0.05$, ** $p < 0.01$, *** $p < 0.001$. One-way ANOVA with Sidak *post hoc* test was used for statistical significance with respect to the growth substrate, with # $p < 0.05$, ### $p < 0.001$, #### $p < 0.0001$.



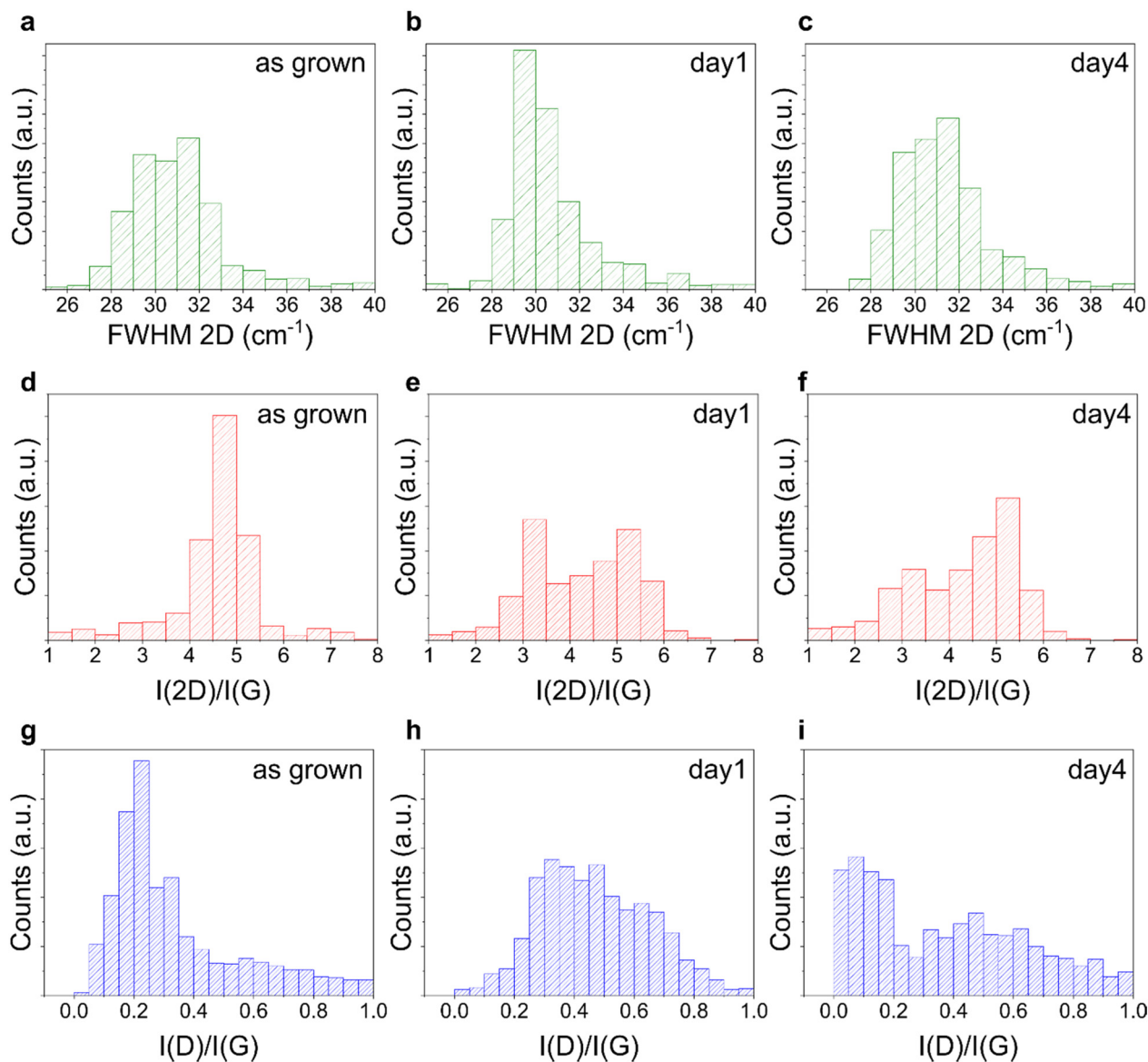


Fig. 3 Raman analysis of graphene on glass before and after treating with neutrophil-like differentiated HL60 for 1 and 4 days. (a–i) Representative histograms obtained from $15 \times 15 \mu\text{m}^2$ Raman maps, showing the (a–c) FWHM of the 2D peak, (d–f) the 2D/G intensity ratio, and (g–i) the D/G intensity ratio, before (a, d and g) and after 1 day (b, e and h) and 4 days (c, f and i) of incubation.

from graphene on SiC and sapphire (Fig. 4b). We observed a similar cell viability for cells cultured on the bare substrates used to grow graphene (SiC and sapphire) and glass control. Also, WS_2 displays a similar cell viability to both glass and sapphire, probably helped by good hydrophilic surfaces that could enhance the early stages of cell adhesion and proliferation, in comparison to hydrophobic surfaces.⁶⁷ Among the graphene-coated samples, those on SiC and on sapphire showed a significant decrease of 16.2 and 23.1% in comparison to the glass control group ($100 \pm 8.9\%$) ($**p < 0.01$ and $***p < 0.001$, respectively) and a decrease in the percentage of viability of 19.6 and 22.4% when compared to the bare substrates on which graphene was grown, namely SiC and sapphire ($^\#p < 0.01$ and $^\#\#\#p < 0.001$, respectively). These variations in cell vi-

bility were, however, not high enough to promote significant variations in the BDNF released by MSCs when incubated with the different substrates (Fig. S10†). A previous study showed a PC12 cell viability on graphene on SiC comparable to that obtained for other controls (glass and SiC).⁷ However, in that work a polymeric coating was used to improve the cell adhesion on the substrates. When an uncoated G SiC Hint was used, cell bodies aggregated and neurite bundles were reported, a clear sign of reduced adhesion.^{7,41} Interestingly, the performance of graphene on SiC was different from that of H-intercalated graphene, our results show a higher viability despite the reduced number of cells (Fig. 4b, G SiC Hint). The reduced MSCs viability on graphene on sapphire confirmed what was previously observed for SH-SY5Y on the same gra-





Fig. 4 (a) MSC cultured on graphene transferred on glass (G glass), graphene on SiC (G SiC), graphene on SiC hydrogen intercalated (G SiC Hint), graphene on sapphire (G sapp), WS₂ on sapphire (WS₂ sapp) and control substrates: glass, SiC and sapphire (Sapp). Scale bars: 100 μ m. (b) Cell viability after 72 hours was tested by MTS assay. The results are reported as percentage versus glass control set to 100%. Data are reported as mean \pm s.e.m. of two independent experiments per substrate. One-way ANOVA with Dunnet *post hoc* test was used for statistical significance with respect to glass control, with ** p < 0.01, *** p < 0.001, and with Šidák *post hoc* test for statistical significance with respect to the growth substrate, with ## p < 0.01, ### p < 0.001.

phene.⁶² Something that these two substrates (*i.e.*, graphene on SiC and graphene on sapphire) have in common, and that differentiates them from the other graphene substrates, is the higher percentage of areas with bilayer thickness. In addition, we noticed that the graphene film on sapphire can be easily

scratched forming graphene debris, resembling the condition of suspended graphene flakes in the cell medium.

In order to study if a loose adhesion to the substrate could affect MSC viability on graphene, cells grown on each sample were then assessed by AFM, to evaluate possible alterations in cell morphologies and topographies (Fig. 5). AFM topographies of fixed MSCs revealed the height of contours of the cell surface. The bright areas identified the elevated parts of the cell, where the nuclei are located. Besides the intrinsic heterogeneity in cell morphology, results evidenced no clear alterations in the shape and morphology of MSCs grown on most of the graphene substrates compared to the glass control. Only the shape of some MSCs on graphene on sapphire seemed more rounded, with shorter protrusions, pointing to a possible reduced cell adhesion (Fig. 5b, G sapp), confirming what was previously observed in Fig. 4a. On the other substrates the cells were mainly spread, showing a healthy and normal shape (Fig. 5b and Fig. S11[†]). The high cell body is clearly visible (green line profiles in Fig. 6), as well as the cell protrusions that extend toward the cells for more than 100 μ m (Fig. 5b, G SiC). A similar morphology was also observed in MSCs grown on the other substrates (Fig. S11[†]). Interestingly, AFM of G on SiC revealed the nanometric terraces of the SiC substrates (Fig. 5b and c, G SiC), which do not influence the cell polarity, with the cell protrusions aligned independently from the direction of the terraces.

Overall, the AFM micrographs revealed a comparable behaviour of MSCs on graphene, with spreading adherent cells. Despite the reduced viability on G SiC, we did not observe considerable cell shape alterations. The cells expressed variable extensions on the substrate, independent of the substrate topography.

Concerning material stability issues, it should be noted that both graphene and WS₂ showed good stability and remained intact during the entire culture period. No visible alterations were observed (Fig. 4a and Fig. S11a, S12[†]), resembling the results previously reported for PC12⁷ and SH-SY5Y⁶² cells.

3.5 Assessment of mitochondrial function on graphene

To explore whether the reduced viability measured by the MTS assay for MSC grown on graphene on SiC and graphene on sapphire is mediated by a mitochondrial instability (which may justify a reduced NADH measured by MTS), we also determined the mitochondrial potential ($\Delta\psi_m$) of MSCs grown on graphene using a fluorescent cationic dye JC-1 (Fig. 6). Indeed, the MTS assay results depend on the mitochondrial electron transport chain; thus, a decreased formazan production could be ascribed to a reduced metabolic activity due to mitochondrial damage. Furthermore, $\Delta\psi_m$ is considered a valuable indicator of cell functional status that helps to evaluate their physiopathological conditions,⁸³ with a decrease in $\Delta\psi$ usually being associated with reduced cell viability and apoptosis.⁸⁴

The mitochondrial activity was evaluated by detecting the red/green fluorescence intensity ratio of JC-1. As shown in Fig. 6a, in the glass control JC-1 emits red fluorescence. After





Fig. 5 Characteristics of MSC morphology on graphene substrates. (a) Morphological images of MSCs after 72 h of culture on glass control and line profiles along the cell body (green) and cell protrusions (red), which are plotted in the near graphs. (b) Morphological images of MSCs grown on graphene on glass (G glass), on SiC (G SiC) and on sapphire (G sapp). Scale bars: 10 μm. (c–e) Line profiles along cell protrusions (c, red), SiC nanometric terraces (d, cyan) and cell body (e, green).

MSC cells were exposed to CCCP (positive control of depolarization), a significant increase in green fluorescence intensity was observed, indicating, as expected, a reduction in $\Delta\psi_m$ ($***p < 0.0001$, Fig. 6b).⁸⁴ Then, the effect of the materials on $\Delta\psi_m$ was investigated. As reported in Fig. 6b, in the control the ratio was 1.97 ± 0.23 . After treatment with CCCP the ratio drastically decreased (0.77 ± 0.26). A significant decrease was also observed in graphene on sapphire ($***p < 0.001$), while the other substrates did not affect the mitochondrial activity.

Overall, the variation in $\Delta\psi_m$ for graphene on sapphire (G sapp, Fig. 6) confirmed what was previously reported in the MTS results. In contrast, no alterations were observed on graphene on SiC, even though this substrate showed a reduced viability similar to graphene on sapphire (Fig. 4). Graphene-

based materials have been shown to alter the stability of mitochondria in different cell models.^{100–102} Xiaoli and coworkers reported an increased mitochondrial stress with a reduction in the membrane potential ($\Delta\psi_m$).¹⁰¹ A positively charged polyethylenimine (PEI)-functionalized GO was also shown to promote mitochondrial fragmentation and cell apoptosis.¹⁰⁰ However, these studies were conducted by incubating the cells with GO or graphene flakes, a completely different condition compared to cells seeded on planar GBMs. As a matter of fact, studies showed the downregulation of neuronal signalling of graphene-exposed neurons, in contrast to the unaltered neuronal activity when seeded on planar graphene, clear proof of the influence of the materials' physical-chemical features on their interaction with the cells.^{103,104}

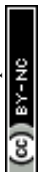




Fig. 6 Evaluation of the mitochondrial potential by JC-1 in MSCs grown on graphene. (a) Representative confocal fluorescence images of MSCs after 4 days of culture, stained with JC-1. Cells on glass were used as the healthy control (Glass). CCCP treated cells were used as positive control of mitochondrial damage (Glass + CCCP). Scale bars: 20 μm . (b) Graph showing the ratio of the intensity of red (JC-1 aggregates) to green (JC-1 monomers) fluorescence. Each value represents the mean intensity ratio of more than 5 fields (200 \times 200 μm^2) per type of substrate of two independent experiments. Data reported as mean \pm s.e.m. One-way ANOVA with Dunnett *post hoc* test vs. glass control, was used for statistical significance, with *** p < 0.001, **** p < 0.0001.

In conclusion, only graphene on sapphire shows poorer cell morphology, reduced cell viability and mitochondrial activity. One could speculate that the lower viability might be induced by small fragments of graphene that could be released by the samples and could be internalized by the cells, with harmful effects. Bilayer graphene is loosely bonded to the substrate and in the presence of a significant number of small bilayer islands, a detachment and internalization of these flakes could indeed negatively affect cell viability. In addition, the debris formed following graphene scratching could release similar flakes with negative effects. Unfortunately, following 24 h incubation with the cell medium, the morphological variations due to medium residuals were comparable to a single layer of graphene thickness and did not allow to appreciate a potential bilayer patch detachment (Fig. S2[†]) and also micro-Raman spectroscopy did not allow us to appreciate variations at the submicrometric scale. Therefore, further studies are necessary to evaluate if other morphological, electrical and/or chemical properties could have impacted the cell behaviour.

4 Conclusion

In order to fully understand the potential of 2D materials for tissue engineering applications, it is critical to explore their interaction with all the cells involved in the process of interest. This is particularly true for the implementation of graphene and the other 2D materials in nerve conduits for peripheral nerve regeneration, where highly different cells (including neurons, Schwann cells, immune cells, stem cells, and fibroblasts) play a role. While the interaction of graphene with nerve cells has been widely explored, less is known about other cells in the context of peripheral nerve injury.¹⁹

Here, first, we assessed the interaction of graphene and WS₂ with neutrophils. Phagocytic cells, such as neutrophils and monocytes, represent the first line of defence against a foreign material and play a critical role in immune response.^{70,105} Among the strategies through which neutrophils eliminate the pathogenic insult, recently it has been reported that neutrophils can extrude NETs, which are mainly composed of DNA and granule proteins.²⁰ The effects of neutrophils on implanted biomaterials vary considerably based on the material used to make implants and the anatomical site of the implant.¹⁰⁵ Neutrophil activation in the first phase of biomaterial implant is pivotal to guarantee the lack of bacterial infection.⁷¹ Notably, excessive neutrophil activation can lead to negative effects. Therefore, their modulation is a key factor to improve tissue-material integration.^{105,106} Keshavan *et al.* discussed the impact of engineered nanomaterials on neutrophils and how neutrophils, in turn, may digest carbon nanotubes and graphene oxide.¹⁹ They also observed that micrometric GO sheets disrupt the lipid rafts in neutrophils and induce the formation of NETs, associated with calcium influx and the production of ROS.⁷³ A similar size-dependency was observed also by Huang and coworkers, who showed how neutrophils gradually degraded GO following two distinct defensive pathways dependent on the dimension of the sheets: NETosis for micrometer-sized flakes or degranulation for nanometer-sized flakes.¹⁰⁷ The degradation mechanism was probably triggered by defects and oxygenated functions on the sheet surfaces, since GO showed faster degradability, when compared to pristine graphene sheets produced by mechanochemical exfoliation.⁷² In view of these considerations, here, we explored if our graphene substrates triggered the release of NETs. We found that graphene and WS₂ were both able to activate NETosis, although the effect was more significant under basal con-



ditions than under conditions in which neutrophils are activated. However, it is worth noting that unlike GO and pristine graphene sheets, our materials were planar and continuous. Only a few nanometric features were present, namely the ridges on graphene on sapphire, formed as a consequence of the different thermal expansion coefficients of graphene and sapphire,⁵⁸ and the atomically flat terraces separated by nanometric steps on graphene on SiC, formed after hydrogen etching of the SiC substrate.^{7,108} However, these features are different from the sharp corners and asperities that characterize the dispersed graphene flakes. Indeed, the flakes have been shown to elicit neutrophil's membrane stripping⁷³ and easily pierce cell membranes, allowing graphene to penetrate the lipid bilayers and interfere with the normal cell function.¹⁰⁹ In agreement with these observations, we found that differently from other graphene forms, our materials were not degraded up to 4 days of incubation with neutrophils. Also, we highlight here the unprecedented observation that pristine graphene may act as a repelling agent for NETs persistence in the injury site, which may be a useful property to exploit for the design of new nerve conduits.

Furthermore, herein, we enriched the details of graphene interactions with MSCs. To date, many studies have reported encouraging results regarding adhesion, proliferation and neuronal differentiation of MSCs on GO, rGO and other graphene-based hybrid materials.^{110,111} All these graphene forms have been extensively used to realize scaffolds, showing improved nerve regeneration and neurite sprouting and outgrowth.^{43,112–116} In contrast, the effect of monolayer CVD graphene on MSCs is still little explored. CVD graphene has been demonstrated to promote the neurogenesis of hMSCs as well as the neurite outgrowths by enhancing MSC–substrate and cell–cell interactions.⁹⁹ However, the majority of the studies focus on the application of CVD graphene in bone tissue engineering for osteogenic differentiation.^{117–119} We focus on CVD and epitaxial graphene, in a relatively pure and flat form, and demonstrate as substrates that are nominally the same material, graphene, but have different effects on MSCs due to their intrinsic properties, a key point in perspective to use graphene in peripheral nerve regeneration. Despite many studies proving that graphene is highly biocompatible,^{7,62,120,121} here graphene on SiC and on sapphire was shown to induce a significant decrease in the viability of MSCs. This, at least for the graphene on sapphire, seems to correlate with a lower mitochondrial activity of the cell and a looser adhesion when they grow on this substrate. Further studies that deepen the knowledge of the surface characteristics and homogeneity of graphene will certainly aid in understanding better the cell–graphene interface that strongly influences the resulting interaction.

Overall, these findings emphasize the importance of choosing the right graphene form to adequately regulate the cell response. The possibility to change and tune graphene properties (*i.e. via* intercalation or functionalization) can provide the possibility to avoid undesirable characteristics and explore the use of graphene as a peripheral neural interface. Indeed,

once the effect of 2D materials on the players involved in nerve regeneration is unravelled, it would be possible to integrate the materials onto a biopolymer support to realize a planar polymeric structure rolled to form tubular nerve conduits. In the literature there are many examples of 3D tubes prepared from a planar scaffold that can be simply rolled along the lengthwise edge and taped,¹²² implanted and wrapped directly around the nerve stumps¹²³ or prepared using self-rolling films.¹²⁴ Similar examples are also between FDA-approved nerve grafts, such as NeuraWrap™ (Integra LifeSciences Co.) that is used by wrapping around the injured nerves, or NeuroMend™ (Collagen Matric, Inc.) that can be unrolled and self-curved to match the dimensions of the injured tissue.

Author contributions

D. C.: conceptualization, investigation, writing – original draft, and visualization; M. N.: conceptualization, investigation, writing – original draft, and visualization; L. R.: conceptualization, investigation, writing – original draft, and visualization; N. M.: investigation and writing – reviewing and editing; V. H.: investigation and writing – reviewing and editing; M. S. B.: investigation and writing – reviewing and editing; L. M.: conceptualization, writing – reviewing and editing, and supervision; C. G.: conceptualization, writing – reviewing and editing, and supervision; M. L. T.: writing – reviewing and editing, and supervision; C. C.: conceptualization, writing – reviewing and editing, and supervision.

Conflicts of interest

There are no conflicts to declare.

Acknowledgements

We acknowledge the support from the University of Pisa under the “PRA – Progetti di Ricerca di Ateneo” (Institutional Research Grants) – Project No. PRA 2020–2021 92 “Quantum Computing, Technologies and Applications”. This work has received funding from the European Union's Horizon 2020 Research and Innovation Programme under grant agreement 881603 and by the Next Generation EU project ECS00000017 ‘Ecosistema dell'Innovazione’ Tuscany Health Ecosystem (THE, PNRR, Spoke 4: Nanotechnologies for Diagnosis and Therapy). This research work is supported also by the “TRITONE project” founded by “Regione Toscana” with “BANDO RICERCA SALUTE 2018”. We thank CISUP at the University of Pisa for the access to the confocal microscopy laboratory facility.

References

- 1 A. Faroni, S. A. Mobasseri, P. J. Kingham and A. J. Reid, *Adv. Drug Delivery Rev.*, 2015, **82**, 160–167.



- 2 R. R. López-Cebral, J. Silva-Correia, R. L. Reis, T. H. Silva and J. M. Oliveira, *ACS Biomater. Sci. Eng.*, 2017, **3**, 3098–3122.
- 3 S. Vijayavenkataraman, *Acta Biomater.*, 2020, **106**, 54–69.
- 4 A. Lavorato, S. Raimondo, M. Boido, L. Muratori, G. Durante, F. Cofano, F. Vincitorio, S. Petrone, P. Titolo, F. Tartara, A. Vercelli and D. Garbossa, *Int. J. Mol. Sci.*, 2021, **22**(2), 572.
- 5 Q. Huang, Y. Cai, X. Zhang, J. Liu, Z. Liu, B. Li, H. Wong, F. Xu, L. Sheng, D. Sun, J. Qin, Z. Luo and X. Lu, *ACS Appl. Mater. Interfaces*, 2021, **13**, 112–122.
- 6 A. C. Pinho, A. C. Fonseca, A. C. Serra, J. D. Santos and J. F. J. Coelho, *Adv. Healthcare Mater.*, 2016, **5**, 2732–2744.
- 7 D. Convertino, S. Luin, L. Marchetti and C. Coletti, *Front. Neurosci.*, 2018, **12**, 1–8.
- 8 L. Scaccini, R. Mezzena, A. De Masi, M. Gagliardi, G. Gambarotta, M. Cecchini and I. Tonazzini, *Int. J. Mol. Sci.*, 2021, **22**, 7901.
- 9 B. E. Fornasari, G. Carta, G. Gambarotta and S. Raimondo, *Front. Bioeng. Biotechnol.*, 2020, **8**, 554257.
- 10 A. J. Petty, R. L. Keate, B. Jiang, G. A. Ameer and J. Rivnay, *Chem. Mater.*, 2020, **32**, 4095–4115.
- 11 D. Convertino, F. Fabbri, N. Mishra, M. Mainardi, V. Cappello, G. Testa, S. Capsoni, L. Albertazzi, S. Luin, L. Marchetti and C. Coletti, *Nano Lett.*, 2020, **20**, 3633–3641.
- 12 N. Li, X. Zhang, Q. Song, R. Su, Q. Zhang, T. Kong, L. Liu, G. Jin, M. Tang and G. Cheng, *Biomaterials*, 2011, **32**, 9374–9382.
- 13 L. Wang, D. Song, X. Zhang, Z. Ding, X. Kong, Q. Lu and D. L. Kaplan, *ACS Biomater. Sci. Eng.*, 2019, **5**, 613–622.
- 14 R. C. Rennert, M. Sorokin, R. K. Garg and G. C. Gurtner, *Regener. Med.*, 2012, **7**, 833–850.
- 15 P. Liu, J. Peng, G. H. Han, X. Ding, S. Wei, G. Gao, K. Huang, F. Chang and Y. Wang, *Neural Regener. Res.*, 2018, 1335–1342.
- 16 A. R. Sas, K. S. Carbajal, A. D. Jerome, R. Menon, C. Yoon, A. L. Kalinski, R. J. Giger and B. M. Segal, *Nat. Immunol.*, 2020, **21**, 1496–1505.
- 17 B. E. Fornasari, M. El Soury, G. Nato, A. Fucini, G. Carta, G. Ronchi, A. Crosio, I. Perroteau, S. Geuna, S. Raimondo and G. Gambarotta, *Cells*, 2020, **9**, 1–19.
- 18 D. Convertino, M.L. Trincavelli, C. Giacomelli, L. Marchetti and C. Coletti, *Front. Bioeng. Biotechnol.*, 2023, **11**, 1–15, DOI: [10.3389/fbioe.2023.1306184](https://doi.org/10.3389/fbioe.2023.1306184).
- 19 S. Keshavan, P. Calligari, L. Stella, L. Fusco, L. G. Delogu and B. Fadeel, *Cell Death Dis.*, 2019, **10**, 569.
- 20 V. Brinkmann, U. Reichard, C. Goosmann, B. Fauler, Y. Uhlemann, D. S. Weiss, Y. Weinrauch and A. Zychlinsky, *Science*, 2004, **303**, 1532–1536.
- 21 J. Wang and H. Arase, *Ann. N. Y. Acad. Sci.*, 2014, **1319**, 66–81.
- 22 N. V. Vorobjeva and B. V. Chernyak, *Biochemistry*, 2020, **85**, 1178–1190.
- 23 E. Kolaczowska and P. Kubes, *Nat. Rev. Immunol.*, 2013, **13**, 159–175.
- 24 O. Soehnlein and L. Lindbom, *Nat. Rev. Immunol.*, 2010, **10**, 427–439.
- 25 K. P. J. M. Van Gisbergen, M. Sanchez-hernandez, T. B. H. Geijtenbeek and Y. Van Kooyk, *J. Exp. Med.*, 2005, **201**, 1281–1292.
- 26 D. Minns, K. J. Smith, G. Hardisty, A. G. Rossi and E. G. Findlay, *Front. Immunol.*, 2021, **12**, 15–17.
- 27 J. A. Marwick, R. Mills, O. Kay, K. Michail, J. Stephen, A. G. Rossi, I. Dransfield and N. Hirani, *Cell Death Dis.*, 2018, **9**, 665.
- 28 E. Frangou, D. Vassilopoulos, J. Boletis and D. T. Boumpas, *Autoimmun. Rev.*, 2019, **18**, 751–760.
- 29 L. Jiang, S. Jones and X. Jia, *Int. J. Mol. Sci.*, 2017, **18**, 1–17.
- 30 C. A. Kubiak, J. Grochmal, T. A. Kung, P. S. Cederna, R. Midha and S. W. P. Kemp, *Muscle Nerve*, 2020, 449–459.
- 31 S. Blando, I. Anchesi, E. Mazzon and A. Gugliandolo, *Int. J. Mol. Sci.*, 2022, **23**(14), 7545.
- 32 M. F. Pittenger, A. M. Mackay, S. C. Beck, R. K. Jaiswal, R. Douglas, J. D. Mosca, M. A. Moorman, D. W. Simonetti, S. Craig and D. R. Marshak, *Science*, 1999, **284**, 143–148.
- 33 T. Sumarwoto, H. Suroto, F. Mahyudin, D. Novembri, D. Tinduh, H. Basuki, C. Rosita, S. Prakoeswa, F. Abdul and S. Rhatomy, *Ann. Med. Surg. (Lond)*, 2021, **67**, 102482.
- 34 X. Li, Y. Guan, C. Li, T. Zhang, F. Meng, J. Zhang, J. Li, S. Chen, Q. Wang, Y. Wang, J. Peng and J. Tang, *Stem Cell Res. Ther.*, 2022, 1–13.
- 35 Y. Chen, L. Xiang, J. Shao and R. Pan, *J. Cell. Mol. Med.*, 2010, **14**, 1494–1508.
- 36 L. Crigler, R. C. Robey, A. Asawachaicharn, D. Gaupp and D. G. Phinney, *Exp. Neurol.*, 2006, **198**, 54–64.
- 37 S. Grijalvo and D. Díaz, *Neurochem. Int.*, 2021, **147**, 105005.
- 38 T. Aydin, C. Gurcan, H. Taheri and Y. Açelya, *Cell Biol. Transl. Med.*, 2018, **3**, 129–142.
- 39 D. Convertino, L. Marchetti and C. Coletti, in *Silicon Carbide Technology for Advanced Human Healthcare Applications*, ed. S. E. Sadow, Elsevier, 2022, pp. 65–98.
- 40 J. S. Lee, A. Lipatov, L. Ha, M. Shekhirev, M. N. Andalib, A. Sinitskii and J. Y. Lim, *Biochem. Biophys. Res. Commun.*, 2015, **460**, 267–273.
- 41 A. Bendali, L. H. Hess, M. Seifert, V. Forster, A. F. Stephan, J. A. Garrido and S. Picaud, *Adv. Healthcare Mater.*, 2013, **2**, 929–933.
- 42 Z. Huang, M. Sun, Y. Li, Z. Guo and H. Li, *J. Mater. Chem. B*, 2021, **9**, 2656–2665.
- 43 J. Wang, W. Zheng, L. Chen, T. Zhu, W. Shen, C. Fan, H. Wang and X. Mo, *ACS Biomater. Sci. Eng.*, 2019, **5**, 2444–2456.
- 44 X. Song, T. Gao, Y. Nie, J. Zhuang, J. Sun, D. Ma, J. Shi, Y. Lin, F. Ding, Y. Zhang and Z. Liu, *Nano Lett.*, 2016, **16**, 6109–6116.
- 45 N. B. Tolou, H. Salimijazi, T. Dikonimos and G. Faggio, *J. Mater. Sci.*, 2021, **56**, 5581–5594.



- 46 Y. Sun, X. Liu, M. N. George, S. Park, B. Gaihre, A. Terzic and L. Lu, *J. Biomed. Mater. Res.*, 2021, 193–206.
- 47 X. Fang, J. Deng, W. Zhang, H. Guo, F. Yu, F. Rao, Q. Li, P. Zhang, S. Bai and B. Jiang, *RSC Adv.*, 2020, **10**, 16769–16775.
- 48 C. Dong, F. Qiao, W. Hou, L. Yang and Y. Lv, *Appl. Mater. Today*, 2020, **21**, 100870.
- 49 S. Lu, W. Chen, J. Wang, Z. Guo, L. Xiao, L. Wei, J. Yu, Y. Yuan, W. Chen, M. Bian, L. Huang, Y. Liu, J. Zhang, Y. Li and L. Jiang, *Small Methods*, 2023, 2200883.
- 50 S. Meng, *Tissue Eng. Regener. Med.*, 2014, **11**, 274–283.
- 51 C. Fu, S. Pan, Y. Ma, W. Kong, Z. Qi and X. Yang, *Artif. Cells, Nanomed., Biotechnol.*, 2019, **47**, 1867–1876.
- 52 J. Wang, Y. Cheng, L. Chen, T. Zhu, K. Ye, C. Jia, H. Wang, M. Zhu, C. Fan and X. Mo, *Acta Biomater.*, 2019, **84**, 98–113.
- 53 M. Bramini, G. Alberini, E. Colombo, M. Chiacchiaretta, M. L. DiFrancesco, J. F. Maya-Vetencourt, L. Maragliano, F. Benfenati and F. Cesca, *Front. Syst. Neurosci.*, 2018, **12**, 1–22.
- 54 J. Li, H. Zeng, Z. Zeng, Y. Zeng and T. Xie, *ACS Biomater. Sci. Eng.*, 2021, **7**, 5363–5396.
- 55 V. Miseikis, D. Convertino, N. Mishra, M. Gemmi, T. Mashoff, S. Heun, N. Haghghian, F. Bisio, M. Canepa, V. Piazza and C. Coletti, *2D Mater.*, 2015, **2**, 014006.
- 56 X. Li, W. Cai, J. An, S. Kim, J. Nah, D. Yang, R. Piner, A. Velamakanni, I. Jung, E. Tutuc, S. K. Banerjee, L. Colombo and R. S. Ruoff, *Science*, 2009, **324**, 1312–1314.
- 57 M. A. Fanton, J. A. Robinson, C. Puls, Y. Liu, M. J. Hollander, B. E. Weiland, M. Labella, K. Trumbull, R. Kasarda, C. Howsare, J. Stitt and D. W. Snyder, *ACS Nano*, 2011, **5**, 8062–8069.
- 58 N. Mishra, S. Forti, F. Fabbri, L. Martini, C. McAleese, B. R. Conran, P. R. Whelan, A. Shivayogimath, B. S. Jessen, L. Buß, J. Falta, I. Aliaj, S. Roddaro, J. I. Flege, P. Bøggild, K. B. K. Teo and C. Coletti, *Small*, 2019, 1904906.
- 59 K. V. Emtsev, A. Bostwick, K. Horn, J. Jobst, G. L. Kellogg, L. Ley, J. L. McChesney, T. Ohta, S. A. Reshanov, J. Röhr, E. Rotenberg, A. K. Schmid, D. Waldmann, H. B. Weber and T. Seyller, *Nat. Mater.*, 2009, **8**, 203–207.
- 60 F. Veliev, A. Briançon-Marjollet, V. Bouchiat and C. Delacour, *Biomaterials*, 2016, **86**, 33–41.
- 61 S. N. Faisal and F. Iacopi, *ACS Appl. Nano Mater.*, 2022, **5**, 10137–10150.
- 62 D. Convertino, N. Mishra, L. Marchetti, M. Calvello, A. Viegi, A. Cattaneo, F. Fabbri and C. Coletti, *Front. Neurosci.*, 2020, **14**, 1–10.
- 63 A. Qu, M. Sun, J. Kim, L. Xu, C. Hao, W. Ma, X. Wu, X. Liu, H. Kuang, N. A. Kotov and C. Xu, *Nat. Biomed. Eng.*, 2021, **5**, 103–113.
- 64 W. Z. Teo, E. L. K. Chng, Z. Sofer and M. Pumera, *Chem. – Eur. J.*, 2014, **20**, 9627–9632.
- 65 A. Murali, G. Lokhande, K. A. Deo, A. Brokesh and A. K. Gaharwar, *Mater. Today*, 2021, **50**, 276–302.
- 66 A. Palumbo, F. Tourlomousis, R. C. Chang and E. H. Yang, *ACS Appl. Bio Mater.*, 2018, **1**, 1448–1457.
- 67 L. Bačáková, E. Filová, F. Rypáček, V. Švorčík and V. Starý, *Physiol. Res.*, 2004, **53**(Suppl. 1), S35–S45.
- 68 J. Luo, Q. Zhou, X. Hu, X. Hou, D. Li, S. Guo and S. Sun, *ACS Appl. Nano Mater.*, 2021, **4**, 10828–10835.
- 69 K. Kostarelos, M. Vincent, C. Hebert and J. A. Garrido, *Adv. Mater.*, 2017, **29**, 1–7.
- 70 S. Jhunjhunwala, *ACS Biomater. Sci. Eng.*, 2018, **4**, 1128–1136.
- 71 S. A. Yavari, S. M. Castenmiller, J. A. G. Van Strijp and M. Croes, *Adv. Mater.*, 2020, 2002962.
- 72 R. Kurapati, S. P. Mukherjee, C. Martín, G. Bepete, E. Vázquez, A. Pénicaud, B. Fadeel and A. Bianco, *Angew. Chem., Int. Ed.*, 2018, **57**, 11722–11727.
- 73 S. P. Mukherjee, B. Lazzaretto, K. Hultenby, L. Newman, A. F. Rodrigues, N. Lozano, K. Kostarelos, P. Malmberg and B. Fadeel, *Chem*, 2017, **4**, 334–358.
- 74 C. Riedl, C. Coletti, T. Iwasaki, A. A. Zakharov and U. Starke, *Phys. Rev. Lett.*, 2009, **103**, 1–4.
- 75 N. Mishra, V. Miseikis, D. Convertino, M. Gemmi, V. Piazza and C. Coletti, *Carbon*, 2016, **96**, 497–502.
- 76 A. Rossi, H. Büch, C. Di Rienzi, V. Miseikis, D. Convertino, A. Al-Temimy, V. Volani, M. Gemmi, V. Piazza and C. Coletti, *2D Mater.*, 2016, **3**, 031013.
- 77 C. L. Frewin, C. Coletti, C. Riedl, U. Starke and S. E. Sadow, *Mater. Sci. Forum*, 2009, **615–617**, 589–592.
- 78 S. J. Martin, J. G. Bradley and T. G. Cotter, *Clin. Exp. Immunol.*, 1990, **79**, 448–453.
- 79 C. Muller, S. Monferran, A. Gamp, P. Calsou and B. Salles, *Oncogene*, 2001, **20**, 4373–4382.
- 80 C. Carmona-Rivera and M. J. Kaplan, *Curr. Protoc. Immunol.*, 2016, 1–14.
- 81 G. Sollberger, B. Amulic and A. Zychlinsky, *PLoS One*, 2016, **11**, 1–10.
- 82 S. T. Smiley, M. Reerstt, C. Mottola-hartshorn, M. Lin, A. Chen, T. W. Smithtt, G. D. Steele and L. B. Chen, *Proc. Natl. Acad. Sci. U. S. A.*, 1991, **88**, 3671–3675.
- 83 A. Perelman, C. Wachtel, M. Cohen, S. Haupt, H. Shapiro and A. Tzur, *Cell Death Dis.*, 2012, **6**, 1–7.
- 84 F. Sivandzade, A. Bhalerao and L. Cucullo, *Bio-Protoc.*, 2019, **9**, 1–13.
- 85 D. Hylane Luiz, A. W. Silveira, M. S. Castro and W. Fontes, *Cells*, 2022, **11**, 2889.
- 86 V. Brunetti, G. Maiorano, L. Rizzello, B. Sorce, S. Sabella, R. Cingolani and P. P. Pompa, *Proc. Natl. Acad. Sci. U. S. A.*, 2010, **107**, 6264–6269.
- 87 L. Erpenbeck, A. L. Gruhn, G. Kudryasheva, G. Günay, D. Meyer, J. Busse, E. Neubert, M. P. Schön, F. Rehfeldt and S. Kruss, *Front. Immunol.*, 2019, **10**, 1–12.
- 88 G. Schönrich and M. J. Raftery, *Front. Immunol.*, 2016, **7**, 11–14.
- 89 K. Martinod and D. D. Wagner, *Blood*, 2014, **123**, 2768–2776.
- 90 E. J. Folco, T. L. Mawson, A. Vromman, B. Bernardes-souza, G. Franck, O. Persson, M. Nakamura, G. Newton,



- F. W. Luscinikas and P. Libby, *Arterioscler. Thromb. Vasc. Biol.*, 2018, **38**, 1901–1912.
- 91 H. Büch, A. Rossi, S. Forti, D. Convertino, V. Tozzini and C. Coletti, *Nano Res.*, 2018, **11**, 5946–5956.
- 92 C. Farrera, K. Bhattacharya, B. Lazzaretto, F. T. Andòn, K. Hulthenby, G. P. Kotchey, A. Star and B. Fadeel, *Nanoscale*, 2014, **6**, 6974–6983.
- 93 V. E. Kagan, N. V. Konduru, W. Feng, B. L. Allen, J. Conroy, Y. Volkov, I. I. Vlasova, N. A. Belikova, N. Yanamala, A. Kapralov, Y. Y. Tyurina, J. Shi, E. R. Kisin, A. R. Murray, J. Franks, D. Stolz, P. Gou, J. Klein-seetharaman, B. Fadeel, A. Star and A. A. Shvedova, *Nat. Nanotechnol.*, 2010, **5**, 1–6.
- 94 S. P. Mukherjee, A. R. Gliga, B. Lazzaretto, B. Brandner, M. Fielden, C. Vogt, L. Newman, A. F. Rodrigues, W. Shao, P. M. Fournier, M. S. Toprak, S. Alexander, K. Kostarelos, B. Kunal and B. Fadeel, *Nanoscale*, 2018, **10**, 1180–1188.
- 95 R. Kurapati, J. Russier, M. A. Squillaci, E. Treossi, C. Ménard-Moyon, A. E. Del Rio-Castillo, E. Vazquez, P. Samori, V. Palermo and A. Bianco, *Small*, 2015, **11**, 3985–3994.
- 96 A. C. Ferrari and D. M. Basko, *Nat. Nanotechnol.*, 2013, **8**, 235–246.
- 97 M. A. Giambra, V. Miseikis, S. Pezzini, S. Marconi, A. Montanaro, F. Fabbri, V. Sorianoello, A. C. Ferrari, C. Coletti and M. Romagnoli, *ACS Nano*, 2021, **15**, 3171–3187.
- 98 K. Kostarelos and K. S. Novoselov, *Science*, 2014, **344**, 261–263.
- 99 J. Kim, S. Park, Y. J. Kim, C. S. Jeon, K. T. Lim, H. Seonwoo, S.-P. Cho, T. D. Chung, P.-H. Choung, Y.-H. Choung, B. H. Hong and J. H. Chung, *J. Biomed. Nanotechnol.*, 2015, **11**, 2024–2033.
- 100 S. Ye, P. Yang, K. Cheng, T. Zhou, Y. Wang, Z. Hou, Y. Jiang and L. Ren, *ACS Biomater. Sci. Eng.*, 2016, **2**, 722–733.
- 101 F. Xiaoli, Z. Yaqing, L. Ruhui, L. Xuan, C. Aijie, Z. Yanli, H. Chen, C. Lili and S. Longquan, *J. Hazard. Mater.*, 2021, **416**, 126158.
- 102 S. Jaworski, B. Strojny, E. Sawosz, M. Wierzbicki, M. Grodzik, M. Kutwin, K. Daniluk and A. Chwalibog, *Int. J. Mol. Sci.*, 2019, **20**(3), 650.
- 103 A. Fabbro, D. Scaini, V. León, E. Vázquez, G. Cellot, G. Privitera, L. Lombardi, F. Torrisi, F. Tomarchio, F. Bonaccorso, S. Bosi, A. C. Ferrari, L. Ballerini and M. Prato, *ACS Nano*, 2016, **10**, 615–623.
- 104 R. Rauti, N. Lozano, V. León, D. Scaini, M. Musto, I. Rago, F. P. Ulloa Severino, A. Fabbro, L. Casalis, E. Vázquez, K. Kostarelos, M. Prato and L. Ballerini, *ACS Nano*, 2016, **10**, 4459–4471.
- 105 G. S. Selders, A. E. Fetz, M. Z. Radic and G. L. Bowlin, *Regener. Biomater.*, 2017, 55–68.
- 106 W. G. Brodbeck, G. Voskerician, N. P. Ziats, Y. Nakayama, T. Matsuda and J. M. Anderson, *J. Biomed. Mater. Res., Part A*, 2003, **64A**, 320–329.
- 107 S. Huang, S. Li, Y. Liu, B. Ghalandari, L. Hao, C. Huang, W. Su, Y. Ke, D. Cui, X. Zhi and X. Ding, *Adv. Healthcare Mater.*, 2022, **11**, 2102439.
- 108 V. Ramachandran, M. F. Brady, A. R. Smith, R. M. Feenstra and D. W. Greve, *J. Electron. Mater.*, 1998, **27**, 308–312.
- 109 Y. Li, H. Yuan, A. von dem Bussche, M. Creighton, R. H. Hurt, A. B. Kane and H. Gao, *Proc. Natl. Acad. Sci. U. S. A.*, 2013, **110**, 12295–12300.
- 110 X. Yao, Z. Yan, X. Wang, H. Jiang, Y. Qian and C. Fan, *Regener. Biomater.*, 2021, 1–9.
- 111 Y. Hui, Z. Yan, H. Yang, X. Xu, W. Yuan and Y. Qian, *ACS Appl. Bio Mater.*, 2022, **5**, 4741–4759.
- 112 A. E. Jakus, E. B. Secor, A. L. Rutz, S. W. Jordan, M. C. Hersam and R. N. Shah, *ACS Nano*, 2015, **9**, 4636–4648.
- 113 Y. Qian, X. Zhao, Q. Han, W. Chen, H. Li and W. Yuan, *Nat. Commun.*, 2018, **9**, 323.
- 114 W. Zhang, X. Fang, Q. Li, W. Pi and N. Han, *Neural Regener. Res.*, 2023, **18**, 200–206.
- 115 X. Liu, A. L. Miller, S. Park, B. E. Waletzki, Z. Zhou, A. Terzic and L. Lu, *ACS Appl. Mater. Interfaces*, 2017, **9**, 14677–14690.
- 116 Y. Qian, X. Wang, J. Song, W. Chen, S. Chen, Y. Jin, Y. Ouyang, Y. Wei-En and C. Fan, *npj Regener. Med.*, 2021, **6**, 31.
- 117 Y. Liu, T. Chen, F. Du, M. Gu, P. Zhang, X. Zhang, J. Liu, L. Lv, C. Xiong and Y. Zhou, *J. Biomed. Nanotechnol.*, 2016, **12**, 1270–1284.
- 118 J. Li, G. Wang, H. Geng, H. Zhu, M. Zhang, Z. Di, X. Liu, P. K. Chu and X. Wang, *ACS Appl. Mater. Interfaces*, 2015, **7**, 19876–19881.
- 119 S. C. Park, W. S. Yang, J. Y. Ahn, J. B. Park, J. Lee, Y. Jung, H. R. Kim, J. Y. Kim, J. M. Lim and B. H. Hong, *2D Mater.*, 2021, **8**, 035012.
- 120 Kenry, W. C. Lee, K. P. Loh and C. T. Lim, *Biomaterials*, 2018, **155**, 236–250.
- 121 I. Lasocka, E. Jastrzębska, L. Szulc-Dąbrowska, M. Skibniewski, I. Pasternak, M. Hubalek Kalbacova and E. M. Skibniewska, *Int. J. Nanomed.*, 2019, **14**, 2281–2299.
- 122 J. Litowczenko, J. K. Wychowaniec, K. Załęski, Ł. Marczak, C. J. C. Edwards-Gayle, K. Tadyszak and B. M. Maciejewska, *Biomater. Adv.*, 2023, **154**, 213653.
- 123 L. Cicero, R. Puleio, G. Cassata, R. Cirincione, L. Camarda, D. Caracappa, L. D'Itri, M. Licciardi and G. E. Vigni, *Polymers*, 2023, **15**, 1–13.
- 124 T. B. Aigner, C. Haynl, S. Salehi, A. O'Connor and T. Scheibel, *Mater. Today Bio.*, 2020, **5**, 100042.

